PTP1B-dependent insulin receptor phosphorylation/residency in the endocytic recycling compartment of CHO-IR cells

Wanda A. Cromlish *, Man Tang, Robert Kyskan, Linda Tran, Brian P. Kennedy

Department of Biochemistry & Molecular Biology, Merck Frosst Centre for Therapeutic Research, Pointe-Claire-Dorval,
P.O. Box 1005, Pointe-Claire-Dorval, Quebec H9R 4P8, Canada

ARTICLE INFO

ABSTRACT

Insulin binds to the α subunit of the insulin receptor (IR) on the cell surface. The insulin–IR complex is subsequently internalized and trafficked within the cell. Endocytosed receptors, devoid of insulin, recycle back to the plasma membrane through the endocytic recycling compartment (ERC). Using a high content screening system, we investigate the intracellular trafficking of the IR and its phosphorylation state, within the ERC, in response to protein tyrosine phosphatase-1B (PTP1B) inhibition. Insulin stimulates, in a time- and dose-dependent manner, the accumulation of phosphorylated IR (pY^{1158,1162,1163} IR) in the ERC of CHO-IR cells. Treatment of CHO-IR cells with PTP1B-specific inhibitors or siRNA leads to dose-dependent increases in IR residency and phosphorylation within the ERC. The results also demonstrate that PTP1B redistributes within CHO-IR cells upon insulin challenge. The established system will allow for efficient screening of candidate inhibitors for the modulation of PTP1B activity.

1. Introduction

Receptor-mediated endocytosis is a biological process by which various macromolecules bind to cell surface receptors, are internalized and trafficked within the cell [1]. The process of receptor-mediated endocytosis has many functional roles. It is involved in the internalization of cytokines and growth factors, regulation of cell-surface receptor expression, antigen presentation and removal of receptor tyrosine kinases from further exposure to ligands in the extracellular milieu [2–4]. Many polypeptide hormones and growth factors, such as insulin, mediate biological effects by binding to their respective cell surface receptors, activating the intrinsic tyrosine kinase and initiating signal transduction pathways that control diverse physiological processes such as cell metabolism, growth, differentiation and proliferation [5,6].

Insulin action is mediated through the insulin receptor (IR), a transmembrane glycoprotein. The IR is synthesized and processed in the endoplasmic reticulum prior to movement of the unactivated IR to the plasma membrane [7]. Binding of insulin to the two α-subunits of IR, localized on the cell surface, leads to a rapid conformational change. This change, an essential step for biological activity, results in the activation of the tyrosine kinase domain, found in the transmembrane ß-subunits [5,6,8–12]. The activated receptor undergoes autophosphorylation on tyrosine residues 1158, 1162, 1163 as well as 972 and is rapidly internalized via clathrin-coated pits, thus leading to very efficient clearance of insulin and its receptor from the cell surface [12–14]. These coated pits invaginate, pinch off from the plasma membrane and form coated vesicles. The clathrin coat dissembles leaving the insulin–IR complex in a membrane bound vesicle, called the endosome [15]. Endocytosis of the activated IR concentrates them within endosomes and allows the IR tyrosine kinase to phosphorylate substrates that are spatially distinct from those accessible at the plasma membrane [13].

Endosomes can be divided into two broad categories: early and late endocytic compartments [4]. Early endosomes are responsible for dissociating and sorting ligands from receptors in an environment that minimizes the risk of damaging receptors to be recycled [16]. Acidification of the endosome by an ATP-dependent proton pump facilitates the release of most ligands from their receptor [15]. The early endosome system can be further divided into sorting endosomes and endocytic recycling compartments (ERCs). Sorting endosomes contain molecules to be recycled, or ligands and receptors that will be degraded, whereas ERCs lack molecules to be degraded [4]. The ERC is found perinuclear and embedded in the microtubule organizing center. Recycled receptors are biologically active, being more responsive and sensitive to subsequent insulin stimulation than ligand-naïve receptors [17]. These IR-mediated events have been documented with EC_{50} values of ~1–10 nM and maximal responses at 100 nM [18,19].

Protein tyrosine phosphatases (PTPs; EC 3.1.3.48), most significantly PTP1B, have been implicated in the negative regulation of insulin action through dephosphorylation of the IR [9]. *In vitro*, PTP1B associates with tyrosine residues 1162 and 1163 of the IR [20–22]. Many other studies have linked PTP1B action to the insulin receptor [22–25]. Compelling data also comes from PTP1B knockout mice, which displayed increased insulin sensitivity in a tissue specific manner [26,27]. Enhanced tyrosine phosphorylation of the IR was observed in muscle and liver, suggestive that the receptor may be a direct substrate of PTP1B [26].

A question arises however, as to the spatiotemporal regulation of IR dephosphorylation, since the IR is localized on the plasma membrane and interacts with an endoplasmic reticulum (ER) localized PTP1B. Recent studies indicate that PTP1B may attenuate the activity of newly synthesized receptor protein tyrosine kinases, as well as controlling the phosphorylation of the receptor in a compartment near the endoplasmic reticulum [28–31]. Little is known about the intracellular interaction of IR and PTP1B. Using the Arrayscan®II, a high content screening (HCS) technology, we characterize and quantify the temporal and spatial dynamics of IR, phosphorylated IR (pY^{1158,1162,1163} IR) and PTP1B within the cellular environment, particularly in the ERC of CHO-IR cells. CHO-IR cells are a heterologous expression system where human insulin receptors are overexpressed in Chinese hamster ovary cells. CHO-IR cells express approximately 1.2×10^6 human IR per cell, whereas CHO cells express approximately 3000 endogenous receptors [32]. CHO and CHO-IR cells also express PTP1B as detected by western blot. Insulin stimulated ERC accumulation of IR and pY^{1158,1162,1163} IR was found to be a time- and insulin dose-dependent process. PTP1B was found to redistribute within the cells during the time course of insulin challenge. We also show that PTP1B inhibitors and siRNA led to dose-dependent increases in IR phosphorylation and residency within the ERC, particularly in the absence of insulin, thus showing that inhibition of PTP1B is insulin mimetic. The evaluation and validation of the cellular IR-PTP1B interaction then allowed for the development of an HCS assay for the screening of potential PTP1B inhibitors.
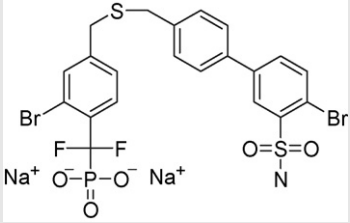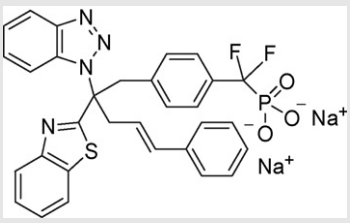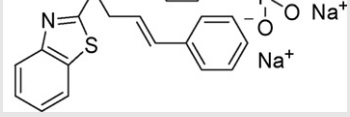
2. Materials and methods
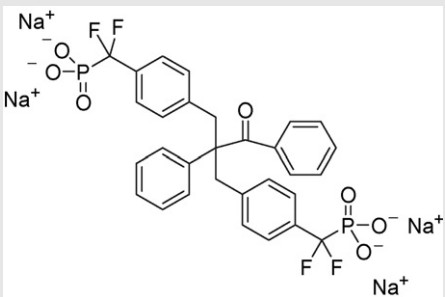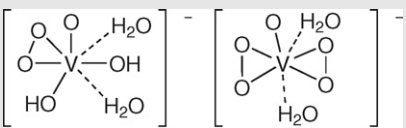
2.1. Reagents

Antibodies were purchased from Upstate Biotechnology (anti-PTP1B), Santa Cruz Biotech (anti-IR) and Biosource International (anti-pY^{1158,1162,1163}-IR). Insulin, bafilomycinA$_1$, colchicine and chloroquine were obtained from Sigma–Aldrich Corp. (St. Louis, MO). Pervanadate, a non-selective protein tyrosine inhibitor and specific PTP1B inhibitors were synthesized at Merck Frosst as described [18,29,33–37] and are shown in Table 1 along with their *in vitro* enzyme potencies. The PTP1B inhibitors are: disodium[{4-[({[3′-(aminosulfonyl)-4′-bromobi-phenyl-4-yl]methyl}thio)methyl]-2-bromophenyl}(difluoro)-methyl]phosphonate (compound 1); disodium[{4-[(4E)-2-(1,3-benzothiazol-2-yl)-2-(1H-1,2,3-benzotriazol-1-yl)-5-phenyl-pent-4-en-1-yl]phenyl}(difluoro)methyl]phosphonate (compounds 2 and 3) and tetrasodium{(2-benzoyl-2-phenyl-propane-1,3-diyl)bis[4,1phenylene(difluoromethylene)]}bis(phosphonate) (compound 4).

2.2. Cell culture

Chinese hamster ovary cells stably overexpressing the insulin receptor (CHO-IR) (Richard Roth, Stanford School of Medicine,

Table 1 – Chemical structures and potency of PTP1B inhibitors

Structure	Compound #	IC50 (nM) (enzymatic assay)	References
	1	8	[29]
	2 3	23 2550	[35]
	4	60	[34]
	Pervanadate	10–50	[18,36,37]

Stanford, CA), were maintained in Ham's F-12 media (Wisent Inc., St. Bruno, QC) supplemented with 10% (v/v) heat-inactivated FBS, 0.1 mg/ml geneticin, 100 U/ml penicillin and streptomycin (Invitrogen Canada Inc., Burlington, ON) at 37 °C in 6% CO_2 humidified atmosphere. For internalization experiments, cells were removed with 0.25% trypsin/EDTA, plated in ClearView 96 well black-walled, clear-bottom microplates (Packard Instrument Co., Meriden, CT) coated with 5 μg/cm^2 fibronectin at $(4–5) \times 10^4$ cells per well.

2.3. Internalization experiments

For time course and insulin dose ranging studies, CHO-IR cells were seeded and attached overnight. The next day, plates were washed three times with warm serum free Ham's F12 media and cells were serum starved for 17 h in this same media. Cells were incubated with concentrations of porcine insulin (24 U/mg, Sigma) ranging from 0 to 1000 μU/ml for 0, 5, 15, 30, 45 or 60 min at 37 °C, 6% CO_2. Cells were washed twice with cold HBSS (Sigma–Aldrich Corp., St. Louis, MO) followed by cellular fixation and nuclear staining.

Compound treatment was performed by preincubating the cells with the designated compound in serum free Ham's F12 media for 1 h prior to insulin treatment. Each agent was present during the insulin stimulation. Cells were washed twice with cold HBSS followed by cellular fixation and nuclear staining.

2.4. Transient transfection with PTP1B siRNA

CHO-IR cells were seeded at 3×10^5 cells per well in six-well plates and attached overnight. Cells were transfected for 2.5 h using Lipofectamine Plus (Invitrogen Canada Inc., Burlington, ON) such that the final concentration of siRNA was 50–200 nM. The antisense sequence of the PTP1B-specific siRNA was 5′GUGUAGUGGAAAUGCAGGA.dT.dT 3′ derived from a target region in the gene that was 100% homologous between human, mouse and rat. The antisense sequence of the non-specific siRNA was 5′AAAGCGAGUGCAUGUGUAUGU.dT.dT. Both siRNA duplexes were 2′-deprotected, purified and used as the desalted form. (Dharmacon Inc., Boulder, CO). The following day, cells were removed from wells using warm

cell dissociation buffer (Specialty Media, Lavallette, NJ). For the ArrayScan internalization studies, 4×10^4 siRNA transfected cells were seeded per ClearView 96 well black-walled, clear-bottomed microplate coated with fibronectin and attached overnight. The cells were serum starved for 17 h followed by insulin stimulation, cellular fixation and nuclear staining. For western blot analysis, the cells from the six-well plates were lysed in T-Per extraction reagent (Pierce Biotechnology Inc., Rockford, IL) containing 100 μM vanadate and protease inhibitors. Samples were loaded on 10% SDS-PAGE gels (Novex Inc., Carlsbad, CA) and then transferred onto nitrocellulose membrane. The levels of PTP-1B were assessed by Western blot.

2.5. Cellular fixation and nuclear staining

CHO-IR cells stimulated with and without insulin were fixed with TBS containing 3.7% formaldehyde for 20 min, permeabilized with 0.1% Triton X-100 for 5 min, and blocked with 5% non-fat milk for 20 min. After blocking, cells were incubated with either a primary antibody to one of the following: 1:200 dilution of anti-IR (α chain); 1:200 dilution of anti-pY[1158,1162,1163] IR or 1:200 dilution of anti-PTP1B for 1 h. Following washes with TBS, incubation with a secondary antibody labeled with FITC (Molecular Probes, Eugene OR) for 1 h was used with each antibody. Antibodies were diluted in 0.1% bovine serum albumin in TBS. For nuclear staining, fixed cells were incubated with 10 μg/ml Hoescht 33342 for 20 min. All labeling procedures were performed at room temperature. Cells were washed twice with HBSS and fresh HBSS was added to each well.

2.6. Data acquisition and analysis

Prepared microplates were loaded onto the ArrayScan®II (Cellomics Inc., Pittsburgh, PA), which is an automated fluorescent imaging microscope used to examine the spatial and temporal distribution of fluorescently labeled components within cells. This system has an inverse optical path that has been optimized for performing rapid automated scans through clear-bottom microplates. It automatically focuses on a field of cells and acquires images in selected fluorescence channels. Individual features, activities and structures of cellular targets or organelles are identified and measured. Results were obtained using application-specific criteria, then tabulated and presented automatically in user-defined formats. All raw data, including images of cells, were archived and available for inspection and analysis. For each well, the 'Receptor Internalization and Trafficking' application reports the number of nuclei (i.e., number of cells) and their area; the number and percentage of cells with the fluorescently labeled component in the ERC; the average and total area of the ERC spots; and the average and total integrated intensities of these spots. In addition, upon visual inspection of acquired images, it was observed that the majority of cells contained one fluorescent ERC per cell and that the ERC size did not differ between treatments. Multiple channels enabled simultaneous quantification of several targets in the same cell or field of cells. Specifically, in our experiments, Hoechst labeled nuclei and FITC-IR, FITC-pY[1158,1162,1163] IR or FITC-PTP1B were measured. In each well, fluorescence arising from Hoechst labeled nuclei (set in the algorithm to display in blue) were used to focus the field and then to determine the cell count in each field. The FITC label fluorescence (set in the algorithm to display red) determined the experimental read-out of accumulation of the biological molecule in the ERC. Image analysis displayed the red spots (ERC) directly adjacent to the blue spots (nuclei).

2.6.1. Statistical analysis
ERC fluorescence for each experimental condition were expressed as the mean of the fold change ± standard error
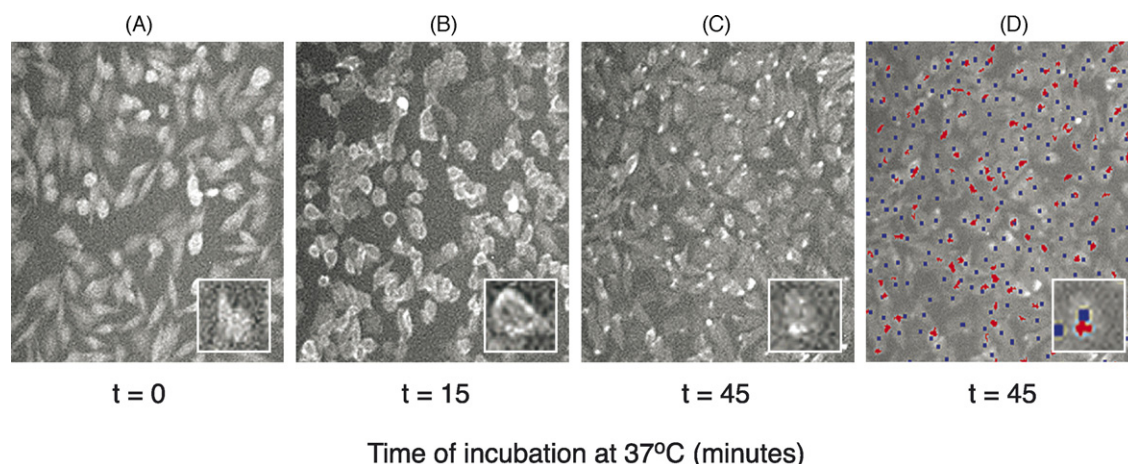
Fig. 1 – Quantitation of insulin induced IR endocytosis into the ERC of CHO-IR cells. Shown are representative fields of IR fluorescence in CHO-IR cells (single cell insert) that were unstimulated (A), stimulated with 50 μU/ml insulin for 15 min (B), or stimulated with 50 μU/ml insulin for 45 min (C and D). Images (A–C) were obtained with the ArrayScan®II before image analysis. Images were acquired on two separate channels of the ArrayScan®II and analyzed for Hoechst 33342-stained nuclei (blue spots) and punctuate perinuclear IR staining (red spots). Image D was obtained following image analysis showing superimposed red and blue spots. Prior to insulin stimulation, only nuclear staining (blue) was visible within each cell. Upon stimulation with insulin, increasing IR (red spots) appears in a perinuclear position.

of the mean (S.E.M.) compared to the control (no treatment) which was set to 1. Where applicable, a Global F-test (one factor, unpaired samples) was used. The data were analyzed via this standard linear model and analysis of variance (ANOVA). P-values less than 0.05 were deemed significant.

3. Results

3.1. Quantification of IR in the ERC of CHO-IR cells in response to insulin

Localization of the IR in unstimulated serum-starved CHO-IR cells revealed membrane surface labelling (Fig. 1A), whereas 15 min of insulin (50 μU/ml) treatment resulted in the IR, within the majority of cells, being found just inside the cell in a concentric fluorescent cytoplasmic ring (Fig. 1B). Following 45 min of insulin stimulation, the cells showed IR fluorescence concentrated into a punctate spot (Fig. 1C). This punctate accumulation of IR in each cell was quantified using the ArrayScan® II Receptor Internalization and Trafficking Algorithm. As well as anti-IR antibody staining, the CHO-IR cells were incubated with Hoechst 33342 to locate the nucleus of all cells in the well. As seen visually in Fig. 1D, the perinuclear localized IR fluorescence (red spots) is shown juxtaposed to the nucleus (blue spots) of each cell. No fluorescence was detected when cells were probed with the secondary antibody alone demonstrating the specificity of the readout (results not shown).

3.2. Effect of endosomal acidotropic agents and receptor trafficking inhibitors on FITC IR accumulation into the ERC

In order to validate that the measured IR fluorescence events were taking place in the ERC, the effect of various endosomal acidotropic agents and receptor trafficking inhibitors on IR accumulation into the ERC was determined. The ERC is embedded in the microtubule organizing center. Colchicine, a microtubule inhibitor, showed no effect on IR accumulation in unstimulated CHO-IR cells, however, upon stimulation with 100 or 1000 μU/ml of insulin for 45 min, there was a significant 60–70% decrease in ERC accumulation (Fig. 2A) ($p < 0.001$). Chloroquine is an acidotropic agent that raises the pH of lysosomes [38]. In these studies, when cells were incubated with chloroquine, no significant difference in IR accumulation into the ERC (Fig. 2B) was observed with or without insulin
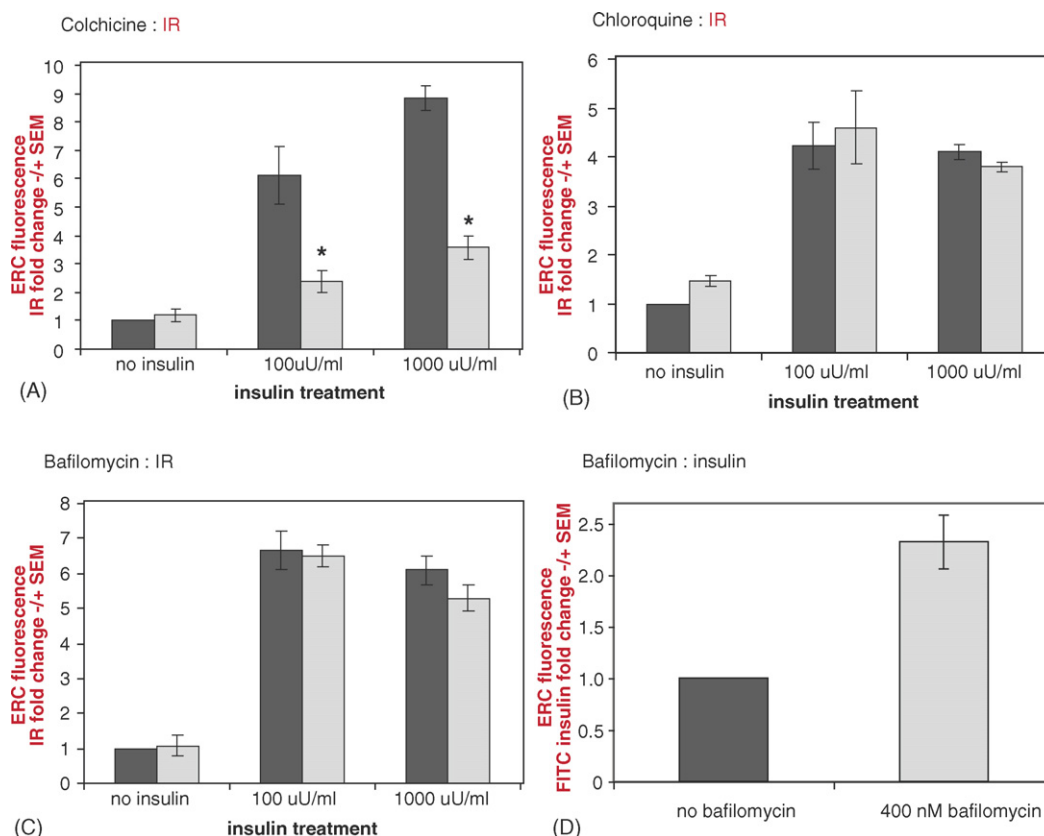

Fig. 2 – Effect of acidotropic and receptor trafficking agents on the accumulation of IR or FITC-insulin in the ERC of CHO-IR cells. CHO-IR cells were preincubated with (▫) or without (▪)10 μM colchicine (A), 500 μM chloroquine (B), or 100 nM bafilomycin (C) for 1 h prior to stimulation with insulin for 45 min. Cells were fixed and stained with anti-IR/FITC antibodies. (D) CHO-IR cells were pre-incubated with (▫) or without (▪) 400 nM bafilomycin then stimulated with FITC-insulin for 45 min. Cells were fixed and ERC fluorescence due to insulin accumulation was measured. Results include three to eight replicates pooled from two experiments. The data were normalized to untreated CHO-IR cells (no insulin, no acidotropic/trafficking agent). The mean fold change in treatment related ERC fluorescence ± standard error of the mean (S.E.M.) is plotted. (*) $p < 0.001$ vs. insulin control.
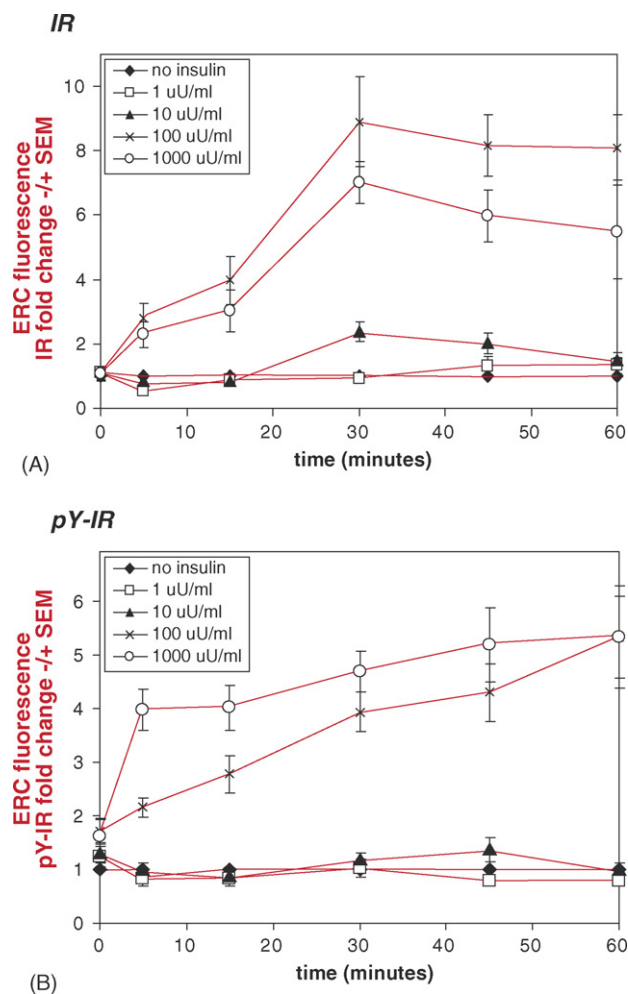
(A)

(B)

Fig. 3 – Time course of IR and pY^{1158,1162,1163}IR accumulation in the ERC of CHO-IR cells. CHO-IR cells were stimulated for 0, 5, 15, 30, 45, 60 min with 0 (◆), 1 (□), 10 (▲), 100 (○), 1000 (×) μU/ml insulin at 37 °C. The cells were fixed and stained with an anti-IR/FITC (A) or anti-pY^{1158,1162,1163}IR/FITC (B) antibodies and Hoechst 33342, then analyzed as described under Section 2. Results include six to nine replicates pooled from two to three experiments for IR and twelve to eighteen replicates pooled from six experiments for pY^{1158,1162,1163}IR. The data were normalized to untreated CHO-IR cells (no insulin) at $t = 0$. The mean fold change in treatment related ERC fluorescence $\pm$ standard error of the mean (S.E.M.) is plotted.
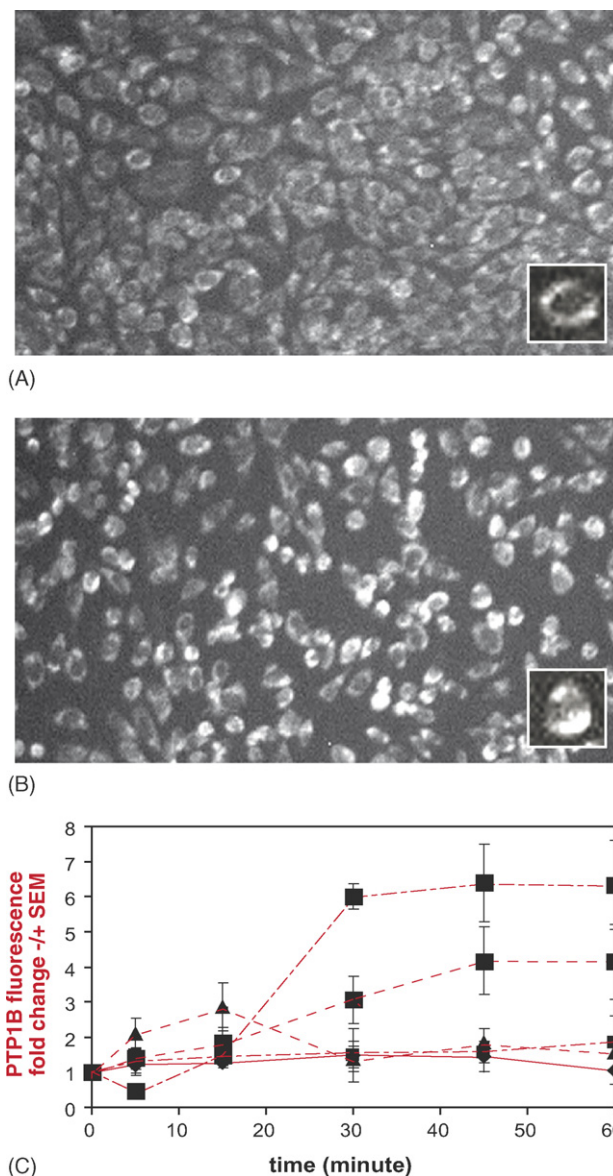

(A)

(B)

(C)

Fig. 4 – Redistribution of intracellular PTP1B-associated fluorescence following insulin stimulation of CHO-IR cells. Shown are representative fields of PTP1B-associated fluorescence in CHO-IR cells (single cell inserts) that were unstimulated (A), or stimulated with 1000 μU/ml insulin for 45 min (B). Images were obtained with the ArrayScan®II before image analysis. (C) CHO-IR cells were stimulated with 0 (◆), 1(■), 10 (▲), 100 (– ■- –), 1000 (-·■·-) μU/ml insulin for 0, 5, 15, 30, 45 or 60 min at 37 °C. The cells were fixed and stained with an anti-PTP1B/FITC antibodies then Hoechst 33342 and analyzed as described under Section 2. Results include six replicates pooled from two experiments. The data were normalized to untreated CHO-IR cells (no insulin) at $t = 0$. The mean fold change in treatment related ERC fluorescence over time $\pm$ standard error of the mean (S.E.M.) is plotted.

stimulation. Internalization of the activated insulin–IR complex leads to the dissociation of insulin from the receptor in the endosomes, followed by ligand degradation in the lysosomes [38]. Using FITC labeled insulin, it was observed that at physiologically relevant concentrations of ligand, only a small percentage of cells (~4% maximum) showed ERC localized FITC labelling. However, when supra-physiological insulin concentrations were used, there was a small increase to 8–16% (data not shown). Preincubation of cells with bafilomycinA$_1$, a selective vacuolar proton pump inhibitor that alkalinizes sorting/recycling endosomes and disrupts the

dissociation of ligand–receptor complexes [39–41], resulted in no change in the accumulation of IR into the ERC in the absence or presence of insulin (Fig. 2C). Interestingly though,
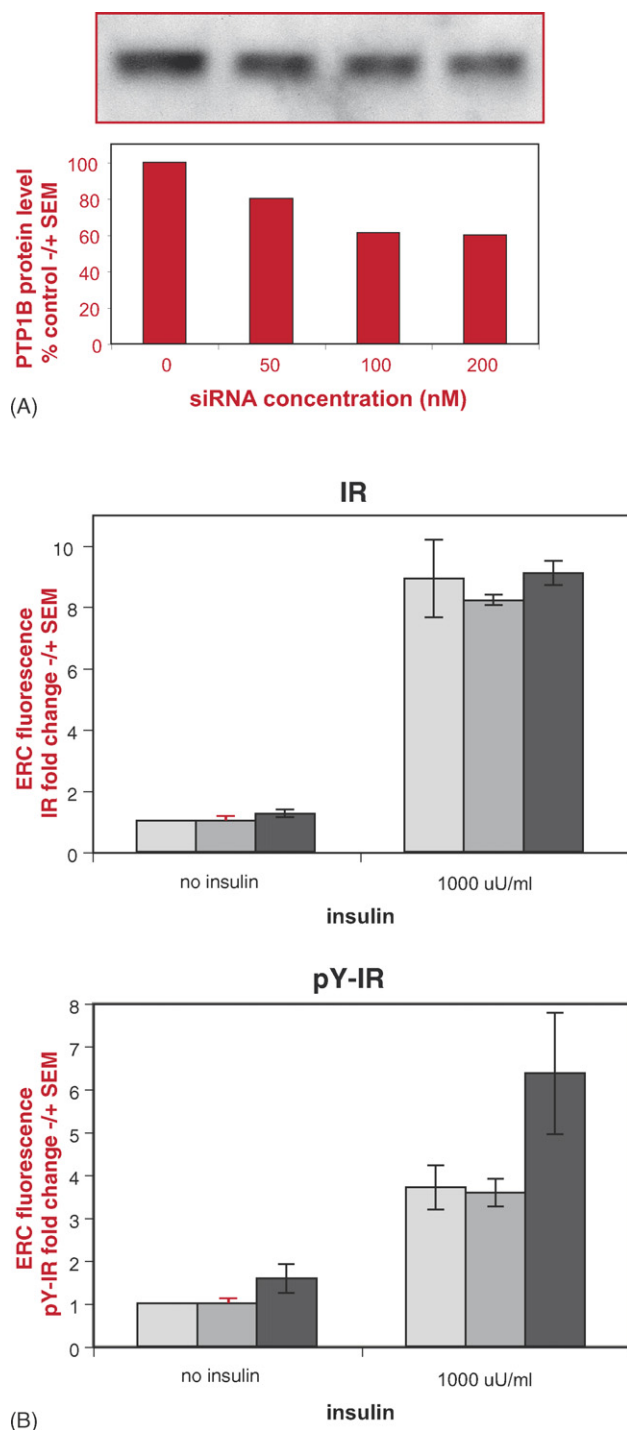
(A)

(B)

Fig. 5 – Effect of PTP1B-specific siRNA on IR phosphorylation and residency in the ERC of CHO-IR cells. Unstimulated CHO-IR cells were transfected with 0 (mock), 50, 100 or 200 nM PTP1B-specific siRNA. (A) Shown is a representative anti-PTP1B western blot and densitometric quantification of PTP1B protein levels from replicate blots. (B) Mock (▢), scrambled (▨) and PTP1B-specific (■) siRNA transfected CHO-IR cells were stimulated with 0 or 1000 μU/ml insulin for 45 min at 37 °C. The cells were fixed and stained with an anti-IR/FITC or anti-pY[1158,1162,1163]IR/FITC antibodies and Hoechst 33342, then analyzed as described under Section 2. Results for IR and

FITC insulin accumulation increased 2.5-fold in the ERC upon bafilomycin treatment (Fig. 2D).

3.3. Time-dependent dose response of insulin induced IR and pY[1158,1162,1163] IR accumulation into the ERC

To define assay parameters such that maximal IR accumulation into the ERC was obtained, CHO-IR cells were stimulated with various concentrations of insulin for up to 60 min. As shown in Fig. 3A, initial IR accumulation into the ERC of CHO-IR cells occurred at 30 min post challenge with 10 μU/ml insulin. A maximal response was obtained following treatment with 100–1000 μU/ml insulin, where a six- to nine-fold increase in IR accumulation was achieved. Analysis of the insulin titration versus IR accumulation into the ERC indicated that an EC_{50} for each time course of $\sim$30 μU/ml was obtained, which corresponds to 0.3 nM or 2 ng/ml insulin (data not shown). These values are comparable to the EC_{50} of 1.4 nM for insulin binding directly on the receptor.

Since insulin stimulation causes phosphorylation and internalization of the IR, the corresponding effect on ERC accumulation of pY[1158,1162,1163] IR was determined. As shown in Fig. 3B, pY[1158,1162,1163] IR accumulated in the ERC rapidly. Maximal accumulation of the pY[1158,1162,1163] IR showed a plateau response of four- to five-fold over unstimulated cells and occurred as early as 5 min post-challenge. An insulin challenge of 100 μU/ml led to a steady time-dependent accumulation of pY[1158,1162,1163] IR in the ERC. Insulin concentrations of 10 μU/ml had little or no effect on the level of pY[1158,1162,1163] IR found in the ERC. For both IR and pY[1158,1162,1163] IR, maximal responses were obtained by 30–60 min. For this reason, a 45 min incubation was typically used for future assays. Interestingly, the number of insulin-stimulated cells with fluorescent staining for IR or pY[1158,1162,1163] IR within the ERC was found to be $\sim$50% of the total cells (data not shown). The responding cell population in these studies is not homogeneous. The cells were cultured using classical methodology for hormonal stimulations, whereby attached and proliferating cells are serum starved to deplete the culture of hormone ligand prior to experimental re-introduction of the ligand. The results demonstrate that using a technology in which data can be obtained on a cell-by-cell basis provides additional information compared to using a total population–response measurement.

3.4. Time course of PTP1B cellular redistribution

As seen visually in Fig. 4A, PTP1B was localized outside of the nucleus in unstimulated CHO-IR cells. This staining is consistent with the known localization of PTP1B in the endoplasmic reticulum. Upon stimulation with 1000 μU/ml

pY[1158,1162,1163]IR include three to six replicates pooled from two experiments for each. The data were normalized to untreated CHO-IR cells (no insulin). The mean fold change in siRNA and insulin related ERC fluorescence ± standard error of the mean (S.E.M.) is plotted.

insulin for 45 min, Fig. 4B showed the redistribution of PTP1B-associated fluorescence within some cells, such that it appeared to concentrate at the ends of the cell. Shown in Fig. 4C, is the quantification of this redistribution as measured by the ArrayScan® II. PTP1B redistributed within the cells following greater than 15 min of insulin stimulation reaching maximal redistribution upon treatment with 1000 μU/ml insulin for 30 min or more. There was no significant change in the localization of PTP1B detected at 1 or 10 μU/ml insulin stimulation up to 60 min.

3.5. Effect of PTP1B siRNA on IR and pY^{1158,1162,1163} IR accumulation into the ERC

Transfection of a PTP1B siRNA into CHO-IR cells led to a dose-dependent decrease in PTP1B, such that 100 and 200 nM siRNA resulted in a 40% decline in PTP1B protein levels compared to controls (Fig. 5A). This maximal reduction in PTP1B levels is small, and may reflect a low rate of PTP1B protein turnover in the CHO-IR cells. To determine whether this reduced level of PTP1B protein had an effect on IR or pY^{1158,1162,1163} IR

accumulation into the ERC, we transfected CHO-IR cells with 200 nM siRNA followed by challenge with 0 or 1000 μU/ml insulin. As seen in Fig. 5B, the knock-down of PTP1B in the absence and presence of insulin did not result in a detectable change in the amount of IR found in the ERC. In contrast to these results, a 40% decrease in PTP1B level in CHO-IR cells affected the level of pY^{1158,1162,1163} IR detected in the ERC. Both in the absence and presence of insulin, approximately a two-fold increase in pY^{1158,1162,1163} IR was observed. Utilization of a scrambled oligo showed no effect, demonstrating that the PTP1B-specific oligo is responsible for the change in pY^{1158,1162,1163} IR levels found in the ERC.

3.6. Effect of PTP1B inhibitors on IR and pY^{1158,1162,1163} IR accumulation into the ERC

The effect of inhibitors of PTP1B on IR and pY^{1158,1162,1163} IR accumulation in the ERC was evaluated. In these series of experiments (Figs. 6–8), data in the absence of insulin is normalized to compound-free, unstimulated cells. Data for insulin challenged cells is presented normalized to maximally
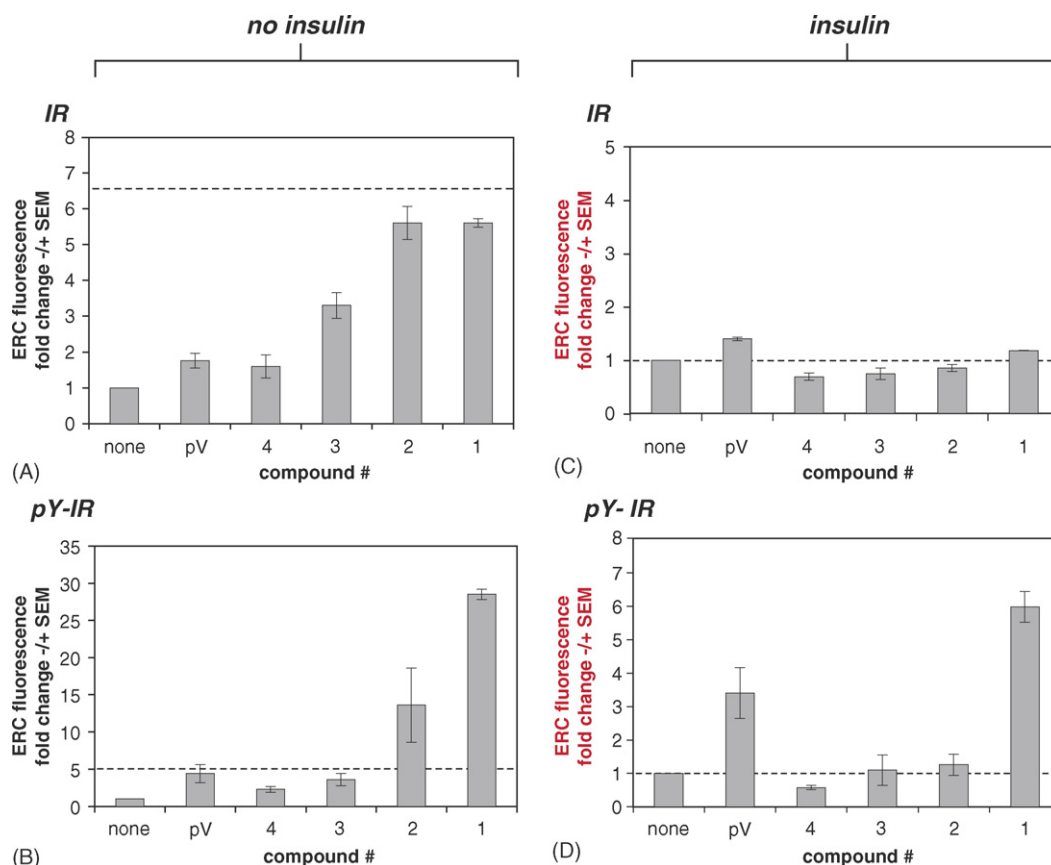

Fig. 6 – Effect of PTP1B inhibitors or pervanadate on IR phosphorylation and residency in the ERC of CHO-IR cells in the absence or presence of insulin. Serum starved CHO-IR cells were preincubated without or with PTP1B-specific compounds at 100–200 μM or pervanadate at 10 μM for 1 h prior to stimulation without (A and B) or with 1000 μU/ml insulin (C and D) for 45 min. Cells were fixed, permeabilized and stained with anti-IR/FITC (A and C) or anti- pY^{1158,1162,1163}IR/FITC (B and D) antibodies and Hoechst 33342, then analyzed as described under Section 2. The data shown are the mean fold change in IR or pY^{1158,1162,1163}IR ERC fluorescence ± standard error of the mean (S.E.M.) for three to six replicates pooled from two experiments. In the absence of insulin, the data is normalized to untreated (no insulin, no compound) cells. In the presence of insulin, the data is normalized to maximally insulin stimulated cells in the absence of compound. The dashed line indicates a maximum response for IR and pY^{1158,1162,1163}IR accumulation in the ERC induced by insulin.

stimulated cells, in the absence of compound. In each of these figures, the dashed line indicates the maximal increase in IR or pY^{1158,1162,1163} IR accumulation found in the ERC, induced by insulin.

Shown in Fig. 6 are the maximal fold changes in ERC localized IR and pY^{1158,1162,1163} IR, in the absence and presence of a maximally stimulating concentration of insulin, for the PTP1B-specific compounds shown in Table 1. The compounds are: (1) disodium[{4-[({[3′-(aminosulfonyl)-4′-bromobiphenyl-4-yl]methyl}thio)methyl]-2-bromophenyl} (difluoro) methyl]-phosphonate; (2 and 3) disodium[{4-[(4E)-2-(1,3-benzothiazol-2-yl)-2-(1H-1,2,3-benzotriazol-1-yl)-5-phenylpent-4-en-1-yl]phenyl}(difluoro)methyl]phosphonate and (4) tetrasodium{(2-benzoyl-2-phenylpropane-1,3- diyl)bis[4,1phenylene(difluoromethylene)]} bis(phosphonate). Pervanadate, a non-selective tyrosine phosphatase inhibitor is also included. In the absence of insulin, pervanadate and the PTP1B-specific compounds, used at individual concentrations that maximally mobilized IR, were able to increase the IR residency (two- to

six-fold) in the ERC (Fig. 6A). All of the compounds evoked increased ERC localized pY^{1158,1162,1163} IR, with the most potent compounds (compounds 1 and 2) able to increase the phosphorylation of the IR to 12- and 30-fold respectively (Fig. 6B). These levels of phosphorylation were three- and six-fold above those, which would be induced by insulin alone. In the presence of insulin, none of the compounds were able to further increase IR residency over and above that stimulated by a maximal insulin challenge (Fig. 6C). Fig. 6D shows that only compound 1 and pervanadate were able to evoke detectable increases in pY^{1158,1162,1163} IR above a maximal insulin stimulated response.

Fig. 7 shows dose–response results for compound 1 (Table 1), the most potent compound tested. In the absence of insulin, increasing concentrations of compound 1 lead to increases in IR accumulation in the ERC, reaching levels equivalent to those stimulated by insulin alone (dashed line in Fig. 7A). The IR found in the ERC was also highly phosphorylated, reaching six-fold greater pY^{1158,1162,1163} IR levels than
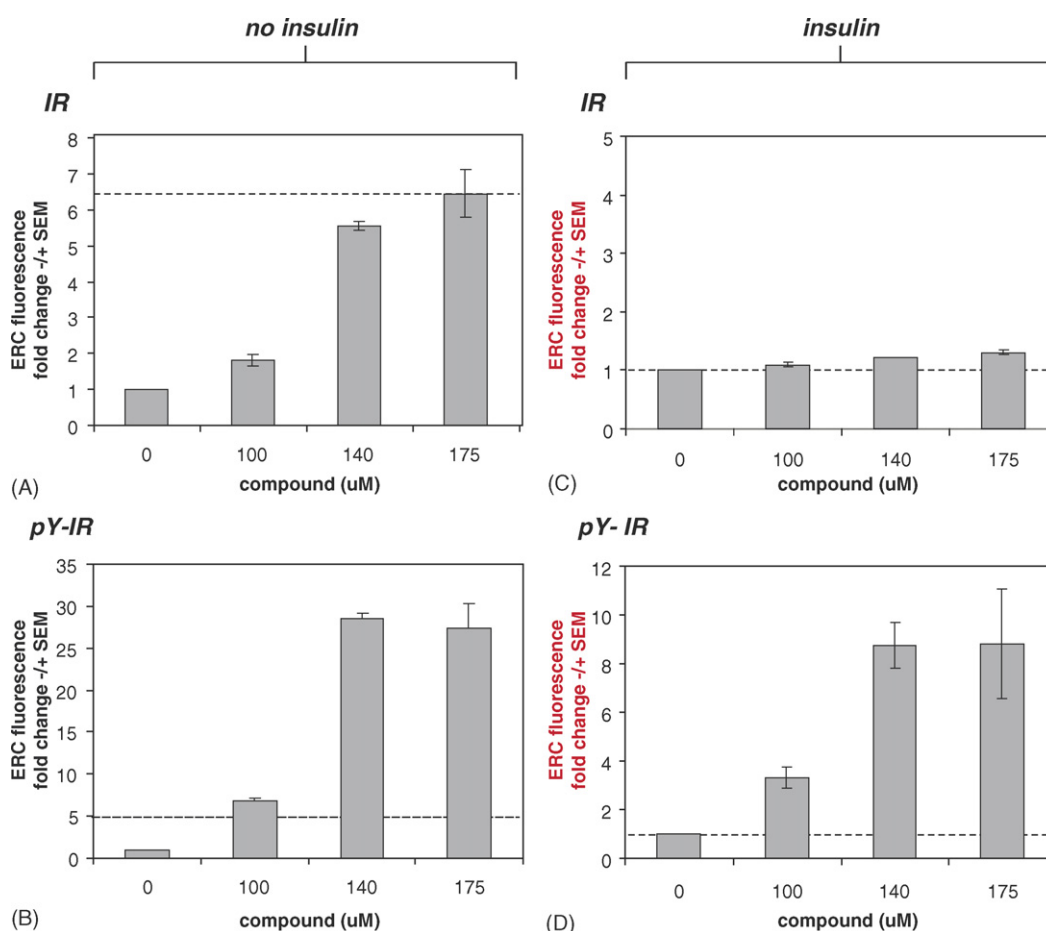

Fig. 7 – Effect of a potent PTP1B inhibitor (compound 1) on IR phosphorylation and residency in the ERC of CHO-IR cells. Serum starved CHO-IR cells were preincubated without or with various concentrations of compound 1 for 1 h prior to stimulation without insulin (A and B) or with 1000 μU/ml insulin(C and D) for 45 min. Cells were fixed, permeabilized and stained with anti-IR/FITC (A and C) or anti- pY^{1158,1162,1163}IR/FITC (B and D) antibodies and Hoechst 33342, then analyzed as described under Section 2. The data shown are the mean fold change in IR or pY^{1158,1162,1163}IR ERC fluorescence ± standard error of the mean (S.E.M.) for three to six replicates pooled from two experiments. In the absence of insulin, the data is normalized to untreated (no insulin, no compound) cells. In the presence of insulin, the data is normalized to maximally insulin stimulated cells in the absence of compound. The dashed line indicates a maximum response for IR and pY^{1158,1162,1163}IR accumulation in the ERC induced by insulin.
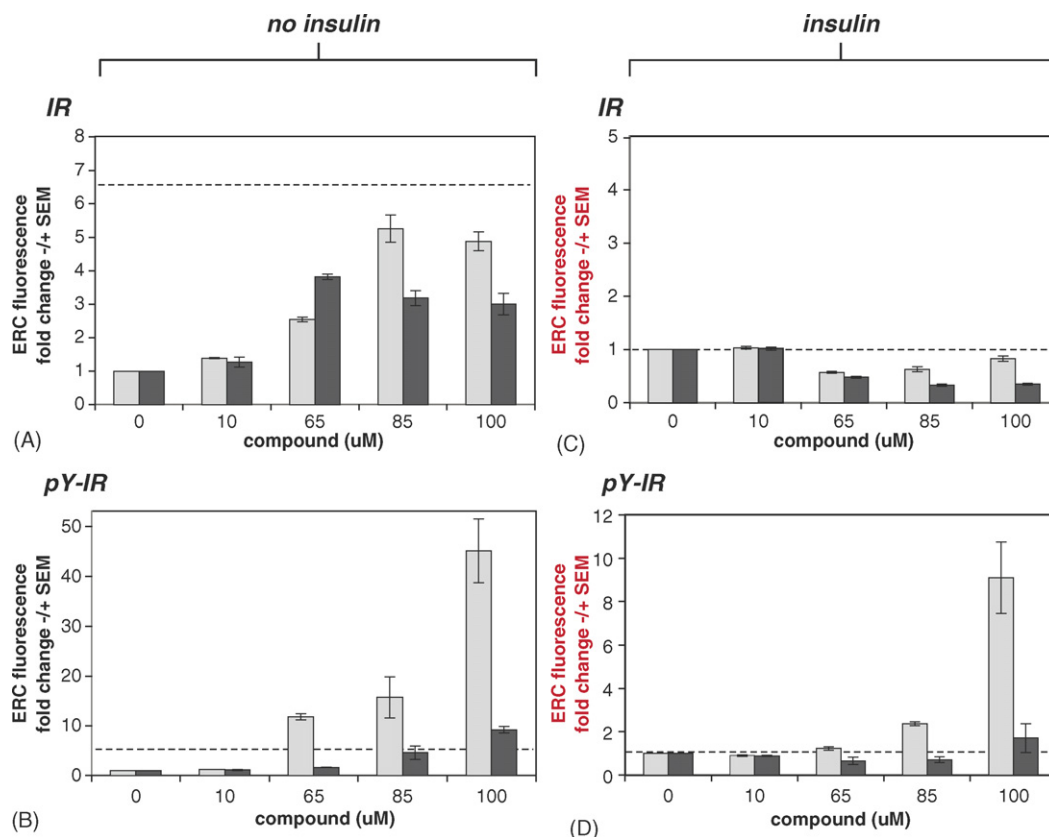
Fig. 8 – Effect of PTP1B enantiomeric inhibitors on IR phosphorylation and residency in the ERC of CHO-IR cells. Serum starved CHO-IR cells were preincubated without or with various concentrations of compound 2 (☐) or compound 3 (■) for 1 h prior to stimulation with (A and B) or without insulin (C and D) for 45 min. Cells were fixed, permeabilized and stained with anti-IR/FITC (A and C) or anti- $pY^{1158,1162,1163}$IR/FITC (B and D) antibodies and Hoechst 33342, then analyzed as described under Section 2. The data shown are the mean fold change in IR or $pY^{1158,1162,1163}$IR ERC fluorescence ± standard error of the mean (S.E.M.) for three to six replicates pooled from two experiments. In the absence of insulin, the data is normalized to untreated (no insulin, no compound) cells. In the presence of insulin, the data is normalized to maximally insulin stimulated cells in the absence of compound. The dashed line indicates a maximum response for IR and $pY^{1158,1162,1163}$IR accumulation in the ERC induced by insulin.

that induced by insulin alone (dashed line in Fig. 7B). In the presence of insulin, compound 1 was able to further stimulate $pY^{1158,1162,1163}$ IR levels (four- to eight-fold) above that evoked by insulin treatment (dashed line in Fig. 7D) however without affecting IR levels in the ERC (Fig. 7C).

Fig. 8 shows data for a benzotriazole enantiomeric pair, in which compound 2 is the active, potent PTP1B inhibitor while compound 3 is non-potent against PTP1B (Table 1). In the absence of insulin, increasing concentrations of the active enantiomer (compound 2), stimulated a five-fold increase in IR (Fig. 8A) and up to a 40 to 50-fold increase in $pY^{1158,1162,1163}$ IR levels found in the ERC (Fig. 8B). The observed $pY^{1158,1162,1163}$ IR reached levels that were nine-fold greater than those stimulated by insulin. The inactive enantiomer (compound 3), although showing the ability to increase IR in the ERC, was as expected, much less potent in promoting $pY^{1158,1162,1163}$ IR accumulation in the ERC (Fig. 8B). In the presence of insulin, neither compound 2 nor compound 3 was able to evoke an influx of receptor (Fig. 8C). However, at high compound concentrations, compound 2 (active enantiomer) was able to further stimulate $pY^{1158,1162,1163}$ IR in the ERC to levels that

were as much as nine-fold over a maximal insulin response (Fig. 8D). The inactive enantiomer had no effect on $pY^{1158,1162,1163}$ IR in the presence of insulin.

4. Discussion

Polypeptide hormones and growth factors form complexes with their receptors, prior to cellular internalization into endosomes. The endosome, in addition to its function in ligand–receptor dissociation, also plays a role in cell signal transduction. First, by attenuating the signaling of the activated cell surface receptor and secondly, by placing the activated receptor in an alternate location to interact with other downstream signaling molecules. The ligand-activated IR is phosphorylated, endocytosed, relieved of insulin and eventually trafficked through the ERC prior to being delivered back to the plasma membrane. PTP1B has been documented to dephosphorylate the IR. In this report, we have used HCS to follow the residency and phosphorylation of the IR in the ERC and have determined the effect of PTP1B inhibition on these

parameters. The CHO-IR cell line was chosen for our studies since the IR is easily detected due to high levels of expression. In addition, CHO-IR cells plate evenly and grow as single cells, an important feature necessary for our studies. Furthermore, numerous studies in the field of endocytosis have been performed using CHO cells. Unlike other cells, they have a single recycling compartment, which is densely concentrated in the pericentriolar region, appearing as a bright spot when viewed by fluorescence microscopy [4,40,42,43]. Previously, the use of HCS technology has focused on the internalization of the transferrin receptor and G-protein coupled receptors [44–46]. Therefore, comparing results, obtained in this study with previous ones, was limited to studies that investigated the kinetics of IR and insulin internalization using a variety of other methods.

Using endosomal acidotropic agents and receptor trafficking inhibitors, we have validated the ArrayScan®II algorithm for IR internalization and trafficking through the ERC. In CHO cells, the tubules of the recycling compartment are condensed around the microtubule organizing center [47]. In this study, colchicine, a microtubule-disrupting agent, significantly decreased IR accumulation into the ERC. Previous studies have demonstrated that colchicine had no effect on ^{125}I-insulin binding to its receptor or internalization of the ligand–receptor complex. It was shown that insulin was delivered to endosomes and lysosomes, but upon colchicine treatment, insulin levels became elevated in the endosomes due to a reduction or delay in the fusion of endosomes with lysosomes [48]. It has also been observed in polarized epithelial cells that translocation of transferrin from the endosomes to the recycling compartment requires actin and microtubules [49]. The observed reduction of IR found in the ERC in this study, would be consistent with colchicine decreasing microtubule function, thus disrupting endosomal trafficking through the recycling compartment. Next, we used the lysosomotropic agent, chloroquine, which is known to neutralize the acidic pH of lysosomes [38,50]. The results show that chloroquine had no effect on the accumulation of IR or its ligand into the recycling endosome of CHO-IR cells. The ERC is a compartment distinct from lysosomes. Previous studies have shown that chloroquine had no effect on IR internalization, inactivation or turnover, but did inhibit the degradation of IR and insulin which had been diverted to the lysosomes, due to alterations in lysosomal hydrolase activities [38]. Finally, bafilomycin A_1 was used to arrest acidification of the endosomal system. Endosomal and lysosomal pH is maintained by vacuolar proton pumps and plays a key role in the dissociation of ligands from receptors, prior to delivery of these endocytosed molecules to late endosomes or lysosomes. Bafilomycin A_1, a macrolide antibiotic, is a selective inhibitor of the vacuolar type H^+-ATPase [39–41]. Within the ERC, a significant 2.5-fold increase of FITC insulin (ligand) was observed in bafilomycin A_1-treated cells, with no change in the level of IR. These results are consistent with a decrease in ligand discharge from the receptor in the endosomal vesicles, with little effect on the recycling pathway, as observed by others in bafilomycin treated cells [51]. The results using colchicine, chloroquine and bafilomycin suggest that the Arrayscan algorithm is indeed quantifying events in the endocytic compartment used for recycling.

The dynamics of the IR and its phosphorylation state, as they traversed the recycling compartment were characterized. Quantification of the ERC-accumulated IR and $pY^{1158,1162,1163}$ IR (activated) was shown to be a time- and insulin dose-dependent process. Steady state IR accumulation into the recycling compartment occurred 30 min post insulin challenge with an EC_{50} of ~0.3 nM (30 μU/ml), implicating a receptor mediated event. Backer et al. incubated serum starved CHO-IR cells with ^{125}I-insulin and showed that the ligand accumulated within the cells, achieving steady state levels after 45 min. They also determined that the processing of insulin occurred at a slower rate in the CHO-IR cells compared to other cell types. It was suggested that since CHO cells have few endogenous insulin receptors, they may not possess the endosomal/lysosomal proteases necessary for rapid insulin processing [52]. Internalization of IR into CHO-IR cells using [^{125}I]-BPA insulin (BPA is a photoactivatable amino acid) which forms a covalent bond with the IR α-subunit upon exposure to UV, showed a similar time course as that obtained in this study, with peak internalization at 20 min followed by a plateau representing the time for recycling of the receptor to the cell surface [32]. Others have shown that the transferrin receptor, known to traverse the ERC, completely cycles through the endosomal system of CHO cells with a $t_{1/2}$ of ~16–24 min [53]. Also consistent with the observed results, DiGuglielmo et al. showed that late endosomes, a compartment immediately upstream of the ERC, accumulated internalized receptor–ligand complexes between 10 and 20 min following ligand binding [5]. Rapid IR internalization into CHO cells requires insulin-induced receptor autophosphorylation [32]. Experiments from this study showed that detectable $pY^{1158,1162,1163}$ IR accumulated in the ERC very rapidly, reaching steady state by 5 min post ligand challenge with high insulin concentrations, a time where ERC detectable IR levels had only begun to increase. Using CHO-IR cells permeabilized with digitonin and pulse-chase techniques, Bernier et al. demonstrated maximal intracellular IR tyrosyl phosphorylation (~five-fold) occurred 2–5 min post insulin stimulation [54]. In the study presented here, maximal IR phosphorylation in the ERC took much longer when 100 μU/ml insulin was used. The reason for this is unclear; however, the level of phosphorylation of the IR is controlled by opposing events. The active phospho-form of IR has an extremely short half-life due to phosphatases removing the phosphate moieties from the receptor, deactivating it and thus terminating insulin action. For insulin concentrations less than 1000 μU/ml, the phosphatases may override the action of the IR kinase.

Faure et al. found that endosomes contain activated IR but no protein tyrosine phosphatase-1B (PTP1B) [55]. Upon ligand binding, the IR-insulin complex has been shown to internalize into endosomal compartments, coming into close proximity with endoplasmic reticulum (ER) localized PTP1B [29,56]. We have observed that in the absence of insulin, PTP1B was found evenly distributed throughout the cytoplasm consistent with ER localization. Upon insulin stimulation, PTP1B measurably redistributed 30 min post challenge. Although most likely associated with insulin-IR internalization, the significance of this observation is unknown, at this time, and will require further exploration.

Galic et al. have demonstrated that PTP1B acts on $pY^{1162/1163}$ IR upon insulin challenge implicating its actions in controlling

the intensity of IR activation and signaling [57]. In the study presented here, changing the activity of PTP1B using either knockdown of PTP1B levels with siRNA or by potently inhibiting its enzymatic activity with inhibitors, resulted in detectable increases in the residency of IR and/or pY^{1158,1162,1163} IR in the ERC. In general, detection of large changes in the pY^{1158,1162,1163} IR levels were proportional to the smaller changes in IR residency. The detectable changes in pY^{1158,1162,1163} IR were on the order of three to five times more sensitive than the IR changes. PTP1B-specific compounds were utilized in these studies, as well as, pervanadate, a non-selective tyrosine phosphatase inhibitor. The potent PTP1B inhibitors (IC$_{50}$ < 60 nM) lead to mobilization of the IR to the ERC and increased levels of phosphorylation of the receptor on tyrosines 1158, 1162 and 1163 in a rank order manner. Compounds 2 and 3 are enantiomeric inhibitors, which are structurally different from the other compounds. They each possess a benzothiazole and a benzotriazole moiety. The results using these two compounds, i.e., compound 3 (weak potency) led to increased IR in the ERC, suggest that they could potentially have off-target activity that is also affecting IR trafficking. The direct comparison of compound 2 versus compound 3 on pY^{1158,1162,1163} IR levels highlights the PTP1B-specific effect. Pervanadate, although a potent inhibitor of PTP1B, also inhibits other tyrosine phosphatases implicated in insulin signaling. These phosphatases could have opposing effects on IR trafficking to the ERC, so the residency of pY^{1158,1162,1163} IR found in this endocytic compartment will be dependent on the cumulative effect of all phosphatases inhibited under the specific stimulus. This most likely explains the observed effects for pervanadate on IR and pY^{1158,1162,1163} IR ERC accumulation. This study showed that, in the absence of insulin, compounds, which potently and specifically inhibit PTP1B led to dose-dependent accumulations of IR, in its phosphorylated form, to be found in the ERC. Thus, PTP1B inhibition showed insulin mimetic properties. In order to have observed these increases in pY^{1158,1162,1163} IR in the ERC in the absence of insulin, PTP1B action must be upstream of the formation of the insulin: IR complex. It has been reported that the co-transfection of IR and PTP1B led to the dephosphorylation of the alpha-beta receptor precursor found in the ER [58,59]. As well Issad et al. observed a basal (insulin-independent) interaction between YFP-PTP1B$_{D181A}$ and IR-*renilla* luciferase [59].

It has been shown that under conditions of high receptor expression, endocytosis is a saturable process, suggesting that there is competition for certain limiting components of the endocytic system [60]. In addition, a default recycling pathway exists for membrane components. The described studies showed that, in the presence of insulin, only the most potent inhibitors evoked additional increases in detectable IR phosphorylation, the sensitivity of IR detection being too low to observe small level changes. Transferrin and other recycling molecules accumulate in the ERC because the rate-limiting step in their return to the surface is the transport from this compartment back to the cell surface [61]. Specific signals are necessary to divert molecules from the recycling compartment. As an example, it has been demonstrated that the C-terminus phosphorylation sites on the human V2 vasopressin receptor, when phosphorylated, prevented the return of the internalized GPCR to the cell surface, thus overriding the natural tendency of the V2 receptor to recycle. It was postulated that dephosphorylation may be the trigger that returns the receptor from the perinuclear compartment to the plasma membrane [62]. PTP1B may also function at the recycling compartment and serve as a trigger to return the IR from the ERC back to the cell surface.

Interestingly, when total IR phosphorylation is followed in CHO-IR cells treated with the compounds used in this study, there was little or no effect on IR phosphorylation above controls (unpublished results). As well, Clampit et al. showed a 50–70% decrease in PTP1B levels using antisense oligos and demonstrated only a two-fold increase in phosphorylated IR as detected by anti-phosphotyrosine antibody [63]. In both of these studies, high background phosphorylation events may have obscured the PTP1B pertinent phosphorylation which occurs in a temporally distinct compartment. The ArrayScan®II technology used in these studies, provides significant advantages over other cell-based applications because HCS can extract information on a cell-by-cell basis rather than providing an average population–response measurement [64] thus allowing biological variability of the cells to be measured. In addition, fluorescent artifacts and background can be isolated and eliminated, while interactions between drug candidates, biomolecules and multiple cellular targets can be monitored in a single HCS assay via multicolour fluorescence that extend over a wide spectral range [64,65]. Complex signaling and feedback pathways within cells can complicate downstream readouts of compound inhibition, however the ArrayScan®II technology provides a highly quantitative, sensitive and reproducible assay readout. Although not presented here, this type of assay readout would allow for other kinetic measures to be made, such as, rate of phosphorylation.

In this manuscript, we describe the characterization and validation of a HCS cell-based assay that quantifies IR residency and phosphorylation in the ERC, as a measure of PTP1B inhibition. Other cell assays to screen for PTP1B inhibitors have previously been developed in Sf9 cells and yeast [66,67]. We show clearly that, compounds from multiple structural classes with nanomolar potencies on PTP1B, as well as PTP1B-specific siRNA, are capable of influencing the residency as well as the phosphorylation level of the IR found in the ERC of CHO-IR cells. This, in turn, could affect the signal transduction emanating from the IR. This report demonstrates that HCS can be used to specifically measure the effects on cellular IR phosphorylation by PTP1B siRNA and inhibitors, and therefore it could be used to efficiently screen for molecules, which inhibit PTP1B activity.

REFERENCES

[1] Schwartz AL. Receptor cell biology: receptor-mediated endocytosis. Pediatr Res 1995;38:835–43.

[2] Brown VI, Greene MI. Molecular and cellular mechanisms of receptor-mediated endocytosis. DNA Cell Biol 1991;10:399–409.

[3] Gill GN. A pit stop at the ER. Science 2002;295:1654–5.

[4] Mukherjee S, Ghosh RN, Maxfield FR. Endocytosis Physiol Rev 1997;77:759–803.

[5] DiGuglielmo GM, Drake PG, Baass PC, Authier F, Posner BI, Bergeron JM. Insulin receptor internalization and signaling. Mol Cell Biochem 1998;182:59–63.

[6] Nystrom FH, Quon MJ. Insulin signaling metabolic pathways and mechanisms for specificity. Cell Signal 1999;11:563–74.

[7] Bass J, Chiu G, Argon Y, Steiner DF. Folding of insulin receptor monomers is facilitated by the molecular chaperones calnexin and calreticulum and impaired by rapid dimerization. J Cell Biol 1998;141:637–46.

[8] Bevan P, Burgess JW, Drake PG, Shaver A, Bergeron JJM, Posner BI. Selective activation of the rat hepatic endosomal insulin receptor kinase. J Biol Chem 1995;270:10784–91.

[9] Drake PG, Posner BI. Insulin receptor-associated protein tyrosine phosphatase(s): role in insulin action. Mol Cell Biochem 1998;182:79–89.

[10] Ottensmeyer FP, Beniac DR, Luo RZ-T, Yip CC. Mechanism of transmembrane signaling: insulin binding and the insulin receptor. Biochemistry 2000;39:12103–12.

[11] White MF, Kahn CR. The insulin signaling system. J Biol Chem 1994;269:1–4.

[12] Perz M, Torlinska T. Insulin receptor-structural and functional characteristics. Med Sci Monit 2001;7:169–77.

[13] Bevan P. Insulin signaling. J Cell Sci 2001;114:1429–30.

[14] Wiley HS, Burke PM. Regulation of receptor tyrosine kinase signaling by endocytic trafficking. Traffic 2001;2:12–8.

[15] Knutson VP. Cellular trafficking and processing of the insulin receptor. FASEB J 1991;5:2130–8.

[16] Mellman I. Endocytosis and molecular sorting. Ann Rev Cell Dev Biol 1996;12:575–625.

[17] Arsenis G, Hayes GR, Livingston JN. Insulin receptor cycling and insulin action in the rat adipocyte. J Biol Chem 1985;260:2202–7.

[18] Fantus IG, Ahmad F, Deragon G. Vanadate augments insulin binding and prolongs insulin action in rat adipocytes. Endocrinology 1990;127:2716–25.

[19] Marshall S. Kinetics of insulin receptor internalization and recycling in adipocytes. J Biol Chem 1985;260:4136–44.

[20] Salmeen A, Andersen JN, Myers MP, Tonks NK, Barford D. Molecular basis for the dephosphorylation of the activation segment of the insulin receptor by protein tyrosine phosphatase 1B. Mol Cell 2000;6:1401–12.

[21] Espanel X, Huguenin-Reggiani M. Van Huijsduijnen RH. The SPOT technique as a tool for studying protein tyrosine phosphatase substrate specificities. Protein Sci 2002;11:2326–34.

[22] Lee JH, Reed DR, Li WD, Xu W, Joo EJ, Kilker RL, et al. Genome scan for human obesity and linkage to markers in 20q13. Am J Hum Genet 1999;64:196–209.

[23] Di Paola R, Frittitta L, Miscio G, Bozzali M, Barratta R, Centra M, et al. A variation in 3′ UTR of hPTP1B increases specific gene expression and associates with insulin resistance. Am J Hum Genet 2002;70:806–12.

[24] Mok A, Cao H, Zinman B, Hanley AJ, Harris SB, Kennedy BP, et al. A single nucleotide polymorphism in protein tyrosine phosphatase PTP1B is associated with protection from diabetes or impaired glucose tolerance in Oji-Cree. J Clin Endocrinol Metab 2002;87:724–7.

[25] Echwald SM, Bach H, Vestergaard H, Richelsen B, Kristensen K, Drivsholm T, et al. A P387L variant in protein tyrosine phosphatase-1B (PTP1B) is associated with type 2 diabetes and impaired serine phosphorylation of PTP1B in vitro. Diabetes 2002;51:1–6.

[26] Elchebly M, Payette P, Michaliszyn E, Cromlish W, Collins S, Loy AL, et al. Increased insulin sensitivity and obesity resistance in mice lacking the protein tyrosine phosphatase-1B gene. Science 1999;283:1544–8.

[27] Klaman LD, Boss O, Peroni OD, Kim JK, Martino JL, Zabolotny JM, et al. Increases energy expenditure, decreased adiposity, and tissue-specific insulin sensitivity in protein-tyrosine phosphatase 1B-deficient mice. Mol Cell Biol 2000;20:5479–89.

[28] Boute N, Boubekeur S, Lacasa D, Issad T. The dissociation and degradation of internalized insulin occur in the endosomes of rat hepatoma cells. EMBO Rep 2003;4:313–9.

[29] Romsicki Y, Reece M, Gauthier J-Y, Asante-Appiah E, Kennedy B. Protein tyrosine phosphatase-1B dephosphorylation of the insulin receptor occurs in a perinuclear endosome compartment in human embryonic kidney 293 cells. J Biol Chem 2004;279:12868–75.

[30] Blanquart C, Boute N, Lacasa D, Issad T. Monitoring the activation state of the insulin-like growth factor-1 receptor and its interaction with PTP1B by using the BRET methodology. Mol Pharmacol 2005;68:885–94.

[31] Haj FG, Verveer PJ, Squire A, Neel BG, Bastiaens PIH. Imaging sites of receptor dephosphorylation by PTP1B on the surface of the endoplasmic reticulum. Science 2002;295:1708–11.

[32] Backer JM, Shoelson SE, Haring E, White MF. Insulin receptors internalize by a rapid saturable pathway requiring receptor autophosphorylation and an intact juxtamembrane region. J Cell Biol 1991;115:1535–45.

[33] Lau CK, Bayly CI, Gauthier J-Y, Li C-S, Therien M, Assante-Appiah E, et al. Structure based design of a series of potent and selective non peptidic PTP1B inhibitors. Bioorg Med Chem Lett 2004;14:1043–8.

[34] Dufresne C, Roy P, Wang Z, Asante-Appiah E, Cromlish W, Boie Y, et al. The development of potent non-peptidic PTP-1B inhibitors. Bioorg Med Chem Lett 2004;14:1039–42.

[35] Scapin G, Patel SB, Becker JW, Wang Q, Desponts C, Waddleton D, et al. The structural basis for the selectivity of benzotriazole inhibitors of PTP1B. Biochemistry 2003;42:11451–9.

[36] Kennedy BP. Role of protein tyrosine phosphatase-1B in diabetes and obesity. Biomed Pharmacother 1999;53:466–70.

[37] Marshall S. Shunting of insulin from a retroendocytotic pathway to a degradative pathway by sodium vanadate. J Biol Chem 1987;262:12005–12.

[38] Knutson VP, Ronnett GV, Lane MD. The effects of cycloheximide and chloroquine on insulin receptor metabolism. J Biol Chem 1985;260:14180–8.

[39] Chinni SR, Shisheva A. Arrest of endosome acidification by bafilomycinA$_1$ mimics insulin action on GLUT4 translocation in 3T3-L1 adipocytes. Biochem J 1999;339:599–606.

[40] Johnson LS, Dunn KW, Pytowski B, McGraw TE. Endosome acidification and receptor trafficking: bafilomycin A$_1$ slows receptor externalization by a mechanism involving the receptor's internalization motif. Mol Biol Cell 1993;4:1251–66.

[41] Presley JR, Mayor S, McGraw TE, Dunn KW, Maxfield FR. BafilomycinA$_1$ treatment retards transferrin receptor recycling more than bulk membrane recycling. J Biol Chem 1997;272:13929–36.

[42] Gruenberg J, Maxfield FR. Membrane transport in the endocytic pathway. Curr Opin Cell Biol 1995;7:552–63.

[43] Presley JF, Mayor S, Dunn KW, Johnson LS, McGraw TE, Maxfield FR. The End2 mutation in CHO cells slows the rate of exit of transferrin receptors from the recycling compartment but bulk membrane recycling is unaffected. J Cell Biol 1993;122:1231–41.

[44] Conway BR, Minor LK, Xu JZ, Gunnet JW, DeBiasio R, D'Andrea MR, et al. Quantification of G-protein coupled receptor internalization using G-protein coupled receptor-green fluorescent protein conjugates with the ArrayScan™ high-content screening system. J Biomol Screen 1999;4: 75–86.

[45] Ding GJF, Fischer PA, Boltz RC, Schmidt JA, Colaiannes JJ, Gough A, et al. Characterization and quantitation of NF-κB nuclear translocation induced by interleukin-1 and tumor necrosis factor-α. J Biol Chem 1998;273:28897–905.

[46] Ghosh RN, Chen Y-T, DeBiasio R, DeBiasio RL, Conway BR, Minor LK, et al. Cell-based, high-content screen for receptor internalization, recycling and intracellular trafficking. Biotechniques 2000;29:170–5.

[47] Marsh EW, Leopold PL, Jones NL, Maxfield FR. Oligomerized transferring receptors are selectively retained by a luminal sorting signal in a long-lived endocytic recycling compartment. J Cell Biol 1995;129:1509–22.

[48] Carpentier RA, Van Obberghen E, Canivet B, Gordon P, Orci L. The endosomal compartment of rat hepatocytes. Its characterization in the course of [^{125}I] insulin internalization. Exp Cell Res 1985;159:113–26.

[49] Apodaca G. Endocytic traffic in polarized epithelial cells: role of actin and microtubule cytoskeleton. Traffic 2001;2:149–59.

[50] Carpentier J-L, Dayer J-M, Lang U, Silverman R, Orci L, Gorden P. Down-regulation and recycling of insulin receptors. J Biol Chem 1984;259:14190–5.

[51] Van Weert AW, Dunn KW, Gueze HJ, Maxfield FR, Stoorvogel W. Transport from late endosomes to lysosomes, but not sorting of integral membrane proteins in endosomes, depends on the vacuolar proton pump. J Cell Biol 1995;130:821–34.

[52] Backer JM, Kahn CR, White MF. The dissociation and degradation of internalized insulin occur in the endosomes of rat hepatoma cells. J Biol Chem 1990;265:14828–35.

[53] Hao M, Maxfield FR. Characterization of rapid membrane internalization and recycling. J Biol Chem 2000;275: 15279–86.

[54] Bernier M, Liotta AS, Kole HK, Shock DD, Roth J. Dynamic regulation of intact and C-terminal truncated insulin receptor phosphorylation in permeabilized cells. Biochemistry 1994;33:4343–51.

[55] Faure R, Baquiran G, Bergeron JJ, Posner BI. The dephosphorylation of insulin and epidermal growth factor receptors. Role of endosome-associated phosphotyrosine phosphatase(s). J Biol Chem 1992;267:11215–21.

[56] Issad T, Boute N, Boubekeur S, Lacasa D. Interaction of PTP1B with the insulin receptor precursor during its biosynthesis in the endoplasmic reticulum. Biochimie 2005;87:111–6.

[57] Galic S, Hauser C, Kahn BB, Haj FG, Neel BG, Tonks NK, et al. Coordinated regulation of insulin signalling by the protein tyrosine phosphatases PTP1B and TCPTP. Mol Cell Biol 2005;25:819–29.

[58] Lammers R, Bossenmaier B, Cool DE, Tonks NK, Schlessinger J, Fischer EH, et al. Diferential activities of protein tyrosine phosphatases in intact cells. J Biol Chem 1993;268:22456–62.

[59] Issad T, Boute N, Perret K. The activity of the insulin receptor assessed by bioluminescence resonance energy transfer. Ann N Y Acad Sci 2002;973:120–3.

[60] Lund KA, Opresko LK, Starbuck C, Walsh BJ, Wiley HS. Quantitative analysis of the endocytic system involved in hormone-induced receptor internalization. J Biol Chem 1990;265:15713–2.

[61] Mayor S, Presley JF, Maxfield FR. Sorting of membrane components from endosomes and subsequent recycling to the cell surface occurs by a bulk flow process. J Cell Biol 1993;121:1257–69.

[62] Innamorati G, Le Gouill C, Balamotis M, Birnbaumer M. The long and short cycle: alternative intracellular routes for trafficking of G-protein-coupled-receptors. J Biol Chem 2001;276:13096–103.

[63] Clampit JE, Meuth JL, Smith HT, Reilly RM, Jirousek MR, Trevillyan JM, et al. Reduction of protein-tyrosine phosphates-1B increases insulin signalling in FAO hepatoma cells. BBRC 2003;300:261–7.

[64] Kapur R. Fluorescence imaging and engineered biosensors. Functional and activity-based sensing using high content screening. Ann N Y Acad Sci 2002;961:196–7.

[65] Liptrot C. High content screening-from cells to data to knowledge. DDT 2001;6:832–4.

[66] Cromlish WA, Payette P, Kennedy BP. Development and validation of an intact cell assay for protein tyrosine phosphatases using recombinant baculoviruses. Biochem Pharmacol 1999;58:1539–46.

[67] Montalibet J, Kennedy BP. Using yeast to screen for inhibitors of protein tyrosine phosphatase 1B. Biochem Pharm 2004;68:1807–14.